Operating Temperature Margin and Heat Load in PF Superconducting Coils of KSTAR

Qiuliang Wang, Cheon Seog Yoon, Jinliang He, Wooho Chung, and Keeman Kim

***Abstract*—The code SAITOKPF has been developed for the design and analysis of the poloidal field (PF) coils system of KSTAR (Korean Superconducting Tokamak Advanced Research) device. The plasma operation is studied by the consideration of the flux conservation. A equivalent circuit model is used to simulate the magnetic coupling among the plasma current, superconducting coils, the tokamak supporting structure and the cryostat. Due to the high changing rates in operating currents of the PF coils, the magnetic coupling can generate high AC losses including the hysteresis loss, the eddy current loss, and the coupling loss. The helium is forced-flowed through the cable in conduit conductor (CICC) to remove the losses and to keep the temperature rise in the superconducting cable lower than its current sharing temperature. The thermal coupling between pancakes, layers, and cooling channels in PF coils is simulated by a quasithree-dimensional thermo-hydraulic model. In this paper, the physical model, the numerical method and the structure of the simulation code are introduced. A nominal operating scenario of KSTAR device is used to simulate these phenomena.**

***Index Terms*—CICC, heat transfer, tokamak PF coil system.**

I. Introduction

THE KSTAR device is a tokamak with a fully superconducting magnet system which enables an advanced quasisteady-state operation. The KSTAR device is designed to run a double-null plasma and also a high-beta single-null plasma at full current [1]. The key design features include long-pulsed operation capability, flexible pressure and current profile control, flexible plasma shape and position control, and advanced profiles and control diagnostics. The major radius of the tokamak is 1.8 m and the minor radius is 0.5 m with the elongation of 2. The KSTAR superconducting magnet system consists of 16 TF coils and 14 PF coils, symmetrically located about the plasma mid-plane. A vacuum cryostat encloses all of the coils. The arrangement of the KSTAR coil system is shown in Fig. 1. 16 TF coils provide 3.5 tesla of the toroidal magnetic field at the plasma center and 14 PF coils provide a flux swing of 16 Volt-seconds. Both of the TF and PF coil system uses internally cooled superconductors. The eight inner PF coils, PF1-4 coils, form the central solenoid (CS) assembly. The CS and PF5 coils use Nb_3Sn strand in Incoloy 908 conduit, while the outer PF coils, PF6-7 coil, use NbTi strand in steinless steel 316 LN conduit. Because the KSTAR mission includes the achievement of extremely long pulse operation at full parameters, the use of superconducting coils is an obvious choice for the magnet system.

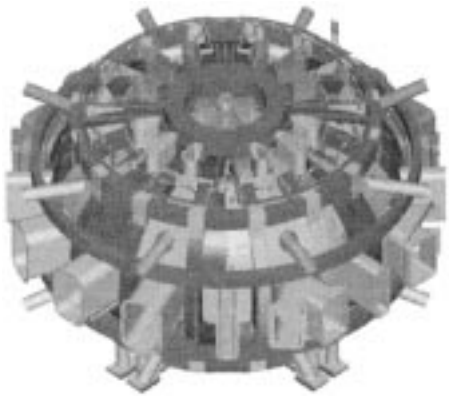

Fig. 1. PF, TF coils, support structures, and vacuum system of KSTAR.

The PF coil system operates in pulsed mode. The PF and TF coils system include coils and the support structure and all components are separated as active and passive circuit. Since the current of the each PF coil varies fast, the inductive current is produced in the active and passive circuits. Due to eddy current losses in passive circuit and AC losses in the superconducting cable of CICC, the helium should remove all heat loads from the structure, superconducting cable, environment, and the conductor itself. Analysis of the PF operation includes the thermal, electromagnetic and fluid coupling. The equivalent circuit model and the quasithree-dimensional thermal hydraulic model are used to simulate the tokamak system. The calculation of coupling, eddy current and hysteresis losses in superconducting cable and the support structure is based on an analytical model. The magnetic coupling circuit equation is solved by unconditionally stable difference methods. The thermal expansion of supercritical helium is described by Navier–Stoke's equation and the equation is solved by the finite element method with the addition of artificial viscosity.

II. Induced Current During Plasma Charging

It is assumed that the decaying time constant of plasma current is greater than that of the passive structure. Therefore, the variation of PF coil current is the independent of detailed plasma behavior and parameters. All superconducting coils are connected with the controlled power supply during normal operating condition with resistivity of $10^{-23}\ \Omega$m. The passive structure and field-correction coils are equivalent to current rings

Manuscript received September 23, 2001. This work was supported by KSTAR project from Korean Ministry of Science and Technology.

Q. Wang, K. Kim, and W. Chung are with the Samsung Advanced Institute of Technology, Taejon-305-380, Republic of Korea (e-mail: qlwang@venus.sait.samsung.co.kr).

J. He is with the Electrical Engineering Department, Tsinghua University, Beijing, P.R. China (e-mail: hejl@tsinghua.edu.cn).

C. S. Yoon is with the Department of Mechanical Engineering, Hannam University, Taejon 306-791 Korea (e-mail: csyoon@mail.hannam.ac.kr).

Publisher Item Identifier S 1051-8223(02)03625-4.

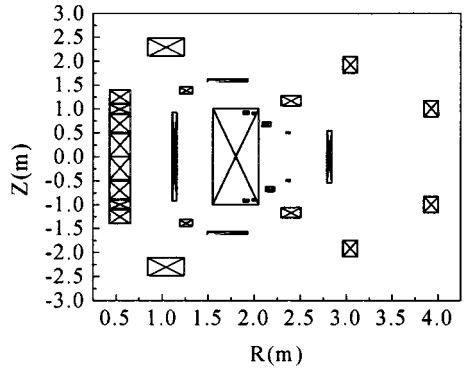

Fig. 2. Equivalent circuit of KSTAR PF and support structure.

with resistance as in Fig. 2. During the variation in PF coil current and plasma current, the equivalent circuit equation for the whole tokamak system is expressed as:

$$\frac{\partial \psi(t)}{\partial t} + I(t)R = V(t),$$

where ψ is the magnetic flux, R denotes the diagonal conductor resistance matrix, I is the vector of the current in the conductor, and V is the vector of the applied voltage in the PF. The coupled, lumped parameter circuit equation for PF system, support structure, and plasma is solved by the linearization of coefficients for the circuit equation using the full-implicit time stepping solution. The initial condition is $I(0) = I_0$. The plasma current goes from 0 to $I_{\max}$ and from $I_{\max}$ to 0, instantaneously. When the plasma current goes from $I_p(0)$ to 0, instantaneously, i.e., the plasma disruption occurs, the current in each PF coil and support structure are calculated with the condition of flux conservation.

III. Helium Thermal Expansion and Transient Heat Removal in Winding Packet of PF Coils

The KSTAR PF coils use CICC in order to obtain high stability, lower AC losses and capacity of supporting to the Lorenz force. One-dimensional model for the helium is reasonable to assume in the thermal hydraulic analysis. Because of the long length of the flow paths, the steady state condition is not established during the single pulse. Thus, a transient thermo-hydraulic analysis is required. The temperatures of helium, strand and conduit are separated in order to simulate the peak temperature rise in the strand. The temperature distribution of the conduit is predicted by the heat conduction equation. The coupled equations for the helium, strand and conduit are expressed as in detail [2]:

$$M\frac{\partial \psi}{\partial t} + A\frac{\partial \psi}{\partial x} + B\psi = \frac{\partial}{\partial x}\left(K\frac{\partial \psi}{\partial x}\right) + G. \qquad (1)$$

The coefficient matrix, $\boldsymbol{K}$, is related to the thermal diffusion term of the superconducting strand and the conduit. The coefficient matrix, $\boldsymbol{A}$, is connected to the convection terms of the supercritical helium, and the coefficient matrix, $\boldsymbol{B}$, denotes the source terms with the function of the variables. The source term, $\boldsymbol{G}$, includes the external thermal load and AC losses. The heat flows, not only along the CICC, but also in transverse direction, through the insulation. Within the pancake-shaped coil, this tends to short-circuit the heat propagation along the conductor causing the pre-heating in adjacent turns. Furthermore, the heat conduction will initiate temperature rise in the adjacent pancakes. Thus, the approximation of the heat transfer in the winding pack is obtained by substituting each part of wire and insulation between two conductors with an equivalent slab having the same average extension in the normal direction to heat flux. By this simplification, the three-dimensional problem is reduced to one-dimensional model [3]. It is noticed that the helium flow changes from the low velocity to the high velocity turbulence flow, and this transition takes place continuously when the heat is gradually increased. It is necessary to add the artificial diffusion term to stabilize the oscillation of the solution. The finite element method with the upwind scheme, which can stabilize the numerical solution of a hyperbolic convection dominated flow problem, is applied to discretize the space terms in governing equation (1) [4].

IV. Heat Load in Superconducting Coils and Support Structure During Normal Operating Tokamak

The high current multi-strand superconducting conductors used in the PF are subjected to the pulsed field. The twisted superconducting strands are not insulated, but they are surrounded with high resistance chrome plated layer. The high field and current changing rate can induce the large AC losses, those can be divided into several constituents: hysteresis, coupling, and eddy losses in the pure strands. All these AC losses superimposed are the total energy deposition in the magnet.

1) Hysteresis Loss in Superconducting Filaments: When a pulse field, B, which is over the penetration field, B_p, penetrates from the outside a round superconducting filament, it reaches to the center of filament. In superconducting strands for the PF, the penetration field is in the range of 10 to 200 mT. It is much lower than the operating field of 7.8 T. While the field change is from $+7.8$ T to -7.8 T, the field may be lower than its penetration field and the hysteresis losses should be calculated according to the field, where the transport current is I_{tr}

$$Q_{hys} = \begin{cases} \dfrac{B^2}{6\mu_0 B_p}\left|\dfrac{dB}{dt}\right|\left(1 - \dfrac{B}{4B_p}\right)A_{non\_Cu} \\ \qquad (B < B_p) \\ \dfrac{2}{3\pi} J_c d_{eff}\left(1 + \dfrac{I_{tr}^2}{I_c^2}\right)\left|\dfrac{dB}{dt}\right| A_{non\_cu} \\ \qquad (B \geq B_p) \end{cases} \quad (\text{W/m}) \qquad (3)$$

where I_C is the critical current of the strands, A_{non_cu} is the cross-sectional area of the superconductor. It is noticed that the critical current density of the superconductor is changed with the local field, temperature and strain. Equation (3) can provide accurate hysteresis loss as a function of the critical current density, J_C, to be assumed as constant. Due to the parallel field, the isotropic of the critical current density is ignored for the hysteresis loss. The hysteresis loss can be calculated on the basis of the following equations with $\beta_s = B_{//}/B_{p//}$, where $B_{//}$

and $B_{p//}$ denote the parallel field and parallel penetration field, repectively.

$$Q_{hs} = \begin{cases} \left|\beta_s M \dfrac{dB}{dt}\right| & (\beta_s \geq 1) \\ \left|\beta_s^3 M \dfrac{dB}{dt}\right| & (\beta_s < 1) \end{cases} \quad \text{(W/m)},$$

$$M = \frac{1}{6} J_c d_{eff} \left(1 + \left(\frac{I_{tr}}{I_C}\right)^2\right) \tag{4}$$

where d_{eff} is the effective filament diameter.

2) Coupling Loss in Superconducting Strands: A variation of the magnetic field induces relatively large coupling current in superconducting strands to generate AC losses. The coupling loss in the strand depends on the coupling time constant, τ_{cp}. If the time scale for magnetic field is much larger than the coupling time constant of strands, the coupling loss in strands is based on the following equation

$$Q_{cp} = \frac{n\tau_{cp}}{\mu_0}\left(\frac{dB}{dt}\right)^2 A_{st} \qquad \text{(W/m)} \tag{5}$$

where n is equal to 2, and A_{st} is the cross sectional area of strands. The current induced by the pulse field among strands also leads to the coupling loss in the multi-stage cable. The coupling time constant depends on the twist pitch of the cable and the transverse resistivity. $n\tau_{cp}$ should be replaced by the coupling time constant in the cable. It is clear that this formula is only valid when all the coupling current time constants are small compared with the field variation time constant. Under this condition, the coupling time constant, $n\tau_{cp}$ of cable is estimated as a summation of N time constant τ_{cp} [4].

3) Eddy Loss in the Pure Copper Strands: The eddy losses in transverse and parallel field are calculated as follows;

$$Q_{eddy} = \begin{cases} \dfrac{R_{st}^2}{4\eta_{cu}}\left(\dfrac{dB_{\perp}}{dt}\right)^2 A_{pure\text{-}Cu} \\ \dfrac{R_{st}^2}{8\eta_{cu}}\left(\dfrac{dB_{//}}{dt}\right)^2 A_{pure\text{-}Cu} \end{cases} \quad \text{(W/m)} \tag{6}$$

where R_{st}, η_{Cu} and $A_{pure\text{-}Cu}$ are the radii, resistivity and cross-sectional area of copper strands, respectively.

4) Eddy Current Losses in the Conduit: If the inner and outer sizes of the conduit are w_i, h_i and w_o, h_o, respectively, the eddy current loss in the conduit due to the transverse field and parallel field are

$$Q_{eddy} = \begin{cases} \dfrac{1}{12\rho_{ss}}\left(w_o^3 h_o - w_i^3 h_i\right)\left(\dfrac{\partial B_{\perp}}{\partial t}\right)^2 \\ \dfrac{1}{90\rho_{ss}}\left[\dfrac{w_o^3 h_o^3}{w_o^2 + h_o^2} - \dfrac{w_i^3 h_i^3}{w_i^2 + h_i^2}\right]\left(\dfrac{\partial B_{//}}{\partial t}\right) \end{cases} \quad \text{(W/m)} \tag{7}$$

where ρ_{ss} is the resistivity of the conduit. The hysteresis loss in the conduit is calculated by the following equation. When the field is lower than 0.25 T, the hysteresis loss is assumed to be zero.

$$Q_{hys\_jk} = \begin{cases} 4100 A_{jk}\left\{\min\left(B_{i+1}, 0.5\right) - \max\left(B_i, -0.5\right)\right\} \\ \qquad B_{i+1} \geq B_i \\ 4100 A_{jk}\left\{\min\left(B_i, 0.5\right) - \max\left(B_{i+1}, -0.5\right)\right\} \\ \qquad B_{i+1} \leq B_i \end{cases} \tag{8}$$

where A_{jk} is the cross-sectional area of the conduit. Generally, the hysteresis and coupling losses in the multi-stage cable are the major loads in CICC.

TABLE I
DIMENSIONS OF PF COILS USED FOR THE CALCULATION

Coil	R(m)	Z(m)	$R_{1(m)}$	$R_{2(m)}$	$Z_{1(m)}$	$Z_{2(m)}$	n_{turns}
PF1, U	0.5499	0.24712	0.42226	0.6775	0	0.49424	180
PF1, L	0.5499	-0.24712	0.42226	0.6775	-0.49424	0	180
PF2,U	0.5499	0.69356	0.42226	0.6775	0.49424	0.89288	144
PF2,L	0.5499	-0.68356	0.42226	0.6775	-0.89288	-0.49424	144
PF3,U	0.5499	0.9966	0.42226	0.6775	0.89288	1.10032	72
PF3,L	0.5499	-0.9966	0.42226	0.6775	-1.10032	-0.89288	72
PF4,U	0.5499	1.25184	0.42226	0.6775	1.10032	1.40336	108
PF4,L	0.5499	-1.25184	0.42226	0.6775	-1.40336	-1.10032	108
PF5,U	1.04915	2.296	0.838	1.2603	2.097	2.495	256
PF5,L	1.04915	-2.296	0.838	1.2603	-2.495	-2.097	256
PF6,U	3.04965	1.92	2.958	3.1413	1.7447	2.0953	84
PF6,L	3.04965	-1.92	2.958	3.1413	-2.0953	-1.7447	84
PF7,U	3.93165	1.000	3.84	4.0233	0.8247	1.1753	84
PF7,L	3.93165	-1.000	3.84	4.0233	-1.1753	-0.8247	84

TABLE II
TF AND PF CONDUCTOR PARAMETERS

Parameter	Units	TF	PF1-5	PF6-7
Conductor		Nb_3Sn	Nb_3Sn	NbTi
Conduit		Incoloy908	Incoloy 908	316LN
Cu/Noncu		1.5:1	1.5:1	3.5:1
$A_{conduit}$	(mm^2)	233	179.2	179.2
D_{strand}	(mm)	0.78	0.78	0.78
$n_{strands}$		486	360	360
$n_{custrands}$		162	120	120
$h_{conduit}$	(mm)	25.65	22.3	22.3
$w_{conduit}$	(mm)	25.65	22.3	22.3
$t_{conduit}$	(mm)	2.86	2.41	2.41
A_{cu}	(mm^2)	179.1	132.7	154.1
A_{noncu}	(mm^2)	65.1	48.25	26.8
A_{Hecond}	(mm^2)	133	111.4	111.4
Lstrand	(km)	3194	1625.8	1563
Lcable	(km)	9.86	6.78	7.33
Mscstrand	(tons)	13.4	6.844	7.5
Ncoils		16	9	4
J_{noncu}	(A/mm^2)	540	544.2	641.8
D_{feff}	(m)	12.5	12.5	10
$E_{hyst_{Noncu}}$ (± 3 T)	(mJ/cc)	250	250	200
n□ (B=0)	(ms)	60	60	60
RRR		100	100	100

V. ANALYSIS OF TEMPERATURE MARGIN AND HEAT LOAD

The basic parameters of superconducting coils for the PF are listed in Table I. The cryogenic cooling parameters for superconducting coils are the inlet pressure of 0.5 MPa and the temperature of 5 K, the outlet pressure of 0.3 Mpa. The parameters of CICC are listed in Table II. The operating margin of the PF magnet system in the KSTAR device strongly depends on the operating scenario for the control of plasma shape. In KSTAR,

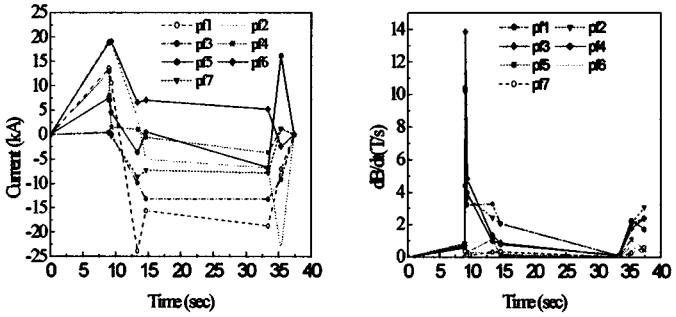

Fig. 3. Operating current and dB/dt in PF coils.

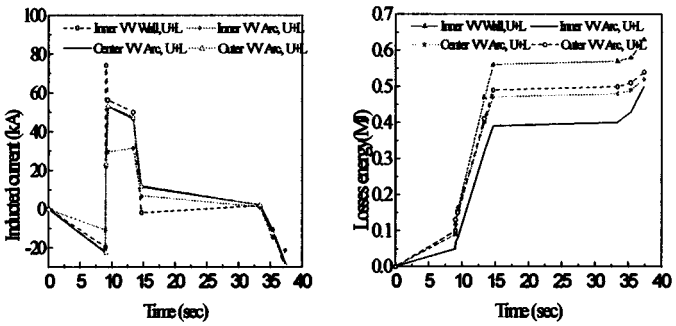

Fig. 4. Induced current and losses energy in the passive structure (VV: vacuum vessel, U: upper, L: lower).

the plasma is controlled by the adjustment of the variation in the PF coil operating current with time. The reference scenario of KSTAR is based on the operating physical requirement.

The reference scenario for the operating currents and the peak field rate with respect to time, dB/dt, for PF coils is plotted in Fig. 3. The total operating time is about 37.36 sec. The variation of the magnetic field determines the amplitude of AC losses in the CICC. The maximum magnetic flux change is over 14 T/s, which occurs at the PF3 coil. The operating margin of the PF coil system depends on the local magnetic field and temperature. The maximum field of about 7.41 T is located at the PF1 coil, and the maximum stored energy of 15.34 MJ is in the PF5 coil. The total stored energy of the KSTAR PF coil system is about 87 MJ. The rapid current variation in the PF coil system induces the eddy current in passive structure and the basic lump circuit equation is solved. The induced current in passive structures of inner vacuum vessel (VV) is plotted in Fig. 4, where the maximum induced current is occurred at the inner vacuum vessel (VV) wall.

The steady state heat loads, such as the losses in the PF structure, losses due to radial and vertical position controller cycling, are not included. All of AC losses and energy deposition are plotted in Fig. 5. The AC coupling loss in the superconducting cable is the main heat load. The thermal hydraulic characteristic in the PF coils is analyzed. Each hydraulic channel goes through one or two double-pancakes, making the inlet and outlet on the same side of the coil winding. Thermal diffusion through the winding pack and flow-splitting through the header are also modeled. After the calculation of the temperature in the conductor at every place and time, the maximum temperatures and minimum operating temperature margin for each coil is plotted in Fig. 6. The maximum temperature rise during the operating scenario is less than 2.5 K. The minimum temperature margin

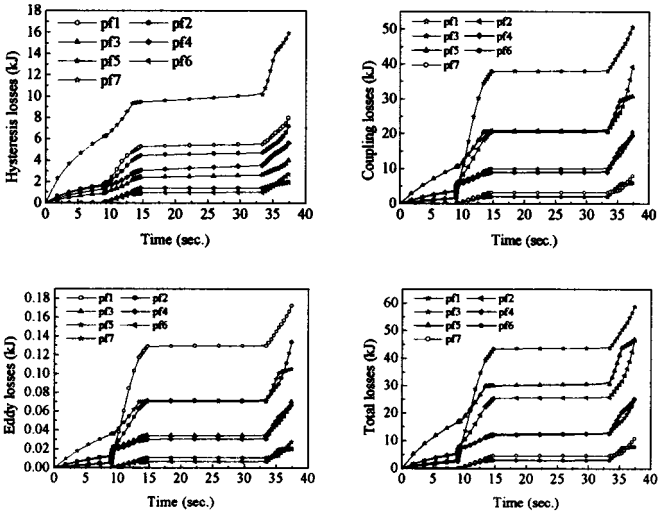

Fig. 5. Hysteresis, coupling, eddy currents and total AC losses in PF coils.

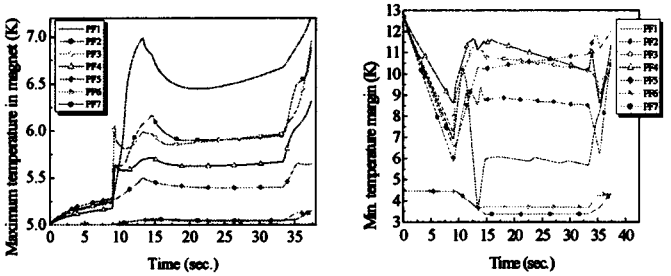

Fig. 6. Maximum temperature rise and temperature margin for PF coils during normal operating scenarios.

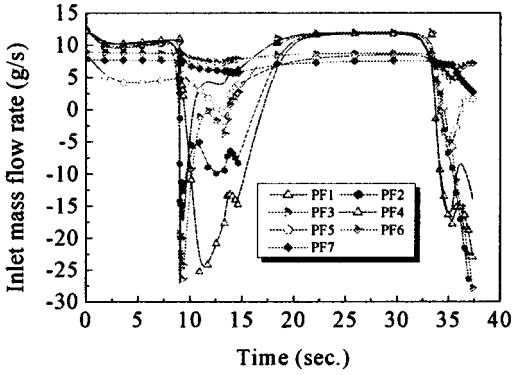

Fig. 7. Inlet mass flow rate with respect to time, during the plasma discharging interval of the KSTAR operating scenario.

of 3.5 K occurs in the PF1 coil. The maximum peak temperature of 6.8 K occurs in the PF5 coil. PF6 and PF7, which use NbTi strand, have a maximum peak temperature of 5.16 K and the minimum temperature margin is about 3.44 K. The helium mass flow rate at the inlet is plotted in Fig. 7.

VI. Conclusions

The thermal analysis of the KSTAR PF coil system according to the operating scenarios has been carried out by the code, SAITOKPF, which calculates the AC losses and cooling self-consistently. The results show that the PF1 has a minimum temperature margin of about 3.5 K and temperature margin of PF7

is about 3.44 K. The major heat load in PF coils is from the AC coupling loss in the multi-stage cable.

REFERENCES

[1] J. H. Schultz, *KSTAR Design Point Definition Workshop*, USA: Princeton Plasma Physics Laboratory, 1997, pp. 205–243.

[2] Q. Wang, S. Oh, K. Ryu, C. Yoon, and K. Kim, "Numerical analysis of stability margin and quench behavior of cable-in-conduit NbTi conductors for KSTAR," *IEEE Trans. Appl. Superconduct.*, vol. 9, no. 2, pp. 620–624, 1999.

[3] L. Bottura and O. C. Zienkiewicz, "Quench analysis of large superconducting magnets," *Cryogenics*, vol. 32, pp. 719–728, 1991.

[4] L. Bottura, "A numerical model for the simulation of quench in the ITER magnets," *J. Computational Phys.*, vol. 125, pp. 26–41, 1996.